A&A manuscript no.
(will be inserted by hand later)

Your thesaurus codes are:
09 (02.08.1; 02.12.1; 06.07.2; 06.16.2)

ASTRONOMY
AND
ASTROPHYSICS
31.3.2000

Correlative relationships in an inhomogeneous solar atmosphere

A.S. Gadun[1], **A. Hanslmeier**[2], **A. Kučera**[3], **J. Rybák**[3], **and H. Wöhl**[4]

[1] Main Astronomical Observatory of Ukrainian NAS, Goloseevo, 03680 Kiev-127, Ukraine
[2] Institut für Geophysics, Astrophysics and Meteorology, Universitätsplatz 5, A-8010 Graz, Austria
[3] Astronomical Institute, Slovak Academy of Sciences, SK-05960 Tatranská Lomnica, Slovakia
[4] Kiepenheuer-Institut für Sonnenphysik, Schöneckstr. 6, D-79104 Freiburg, Germany

Received date; accepted date

Abstract. Correlative relationships between various quantities of 2-D inhomogeneous time-dependent solar atmospheres obtained from models are analysed. They are found to be directly related to height-dependent correlations obtained from observations of spectrograms. We detect four photospheric regions with thermal convection, overshooting convection, transition layer, and fully oscillating layer. The correlations found for the model data and those computed within simulated spectral scans are a good testing tool for depths of formation in spectral lines if these correlations are analysed in comparison. As an example, we examine two criteria, providing heights of line core formation in LTE, and show that the approach which defines this quantity as geometrical height at line center optical depth $\tau_{\lambda 0} = 1$ is more suitable for diagnostic purpose than the method based on depression contribution function.

Key words: hydrodynamics – line formation – Sun: granulation – Sun: photosphere

1. Introduction

The solar photosphere can be treated as a transition layer between thermal convection, which predominates in the low photosphere and below the surface, and different kinds of oscillations, which completely define the gas dynamics in the upper layers.

This was studied in a large number of papers – for instance, among others, by Leighton et al. (1962), Evans (1964), Krat (1973), Canfield & Mehltretter (1973), Keil & Canfield (1978), Kneer et al. (1980), Durrant & Nesis (1981, 1982), Nesis et al. (1988), Komm et al. (1990, 1991a, 1991b), Karpinsky (1990), Hanslmeier et al. (1990, 1994), Balthasar et al. (1990), Kučera et al. (1995). In the papers of Gadun et al. (1997 and 1999) theoretical spectral scans were used to reproduce and interpret correlative relationships derived from spectral observations. These theoretical spectra were simulated with 2-D models.

In this paper we want to investigate correlative height-dependent relationships between selected quantities of 2-D model atmospheres. These theoretical correlations are derived directly from time-dependent 2-D models. Correlation analysis is the most simple method providing information concerning the global behaviour of physical quantities in the photospheric medium.

To test the ability of spectral observations for their usage for diagnostic purpose we compare theoretical correlations with those following from spectral scans simulated on base of the same 2-D models. We show that the result of this comparison is sensitive to the method providing an estimation of line formation depths and analyse two criteria to calculate them. Finally we test our simulations by comparing theoretical correlations with those obtained from real spectral scans done with high spatial and spectral resolution.

2. 2-D models and spectral observations

The 2-D models used here were described in detail by Gadun et al. (1999). They have a computational box with sizes 3360km×1960km in horizontal and vertical directions (the atmospheric layers occupy about 700 km). The spatial step is 28 km.

2-D models normally produce larger model oscillations than 3-D simulations. Therefore in these simulations special boundary conditions at the top and at the bottom of the computational domain were chosen such that the oscillations were kept as weak as possible. These conditions were described in detail by Gadun et al. (1999) . The total evolution time of simulated granulation which was taken

Send offprint requests to: A. Hanslmeier into consideration in our analysis is about $2^h\ 22.5^m$. The time step between the studied models is 30 s.

The spectral observations were described in detail by Kučera et al. (1995) and Hanslmeier et al. (2000). They were carried out with the Vacuum Tower Telescope (Observatorio del Teide, Tenerife) using its echelle spectrograph. Five Fe I spectral lines have been observed strictly simultaneously with exposure time of 0.3 s: 5434.543 Å, 6494.994 Å, 5576.508 Å, 6301.508 Å, and 6302.499 Å. Their main line characteristics are given in Kučera et al. (1995). The slit width was 0.28″ and each spectral profile corresponded to 0.17″ in the spatial direction. The dispersion of the spectra were between 3.3 and 4.0 mÅ/px. Only the most quiet region covering the slit for 30″ length was used for computation of the spectral line characteristics of the continuum intensity, the residual line core intensity and the Doppler shifts in each spectral profile. This region was without supergranular network activity and was situated close to the disk center ($\mu > 0.95$).

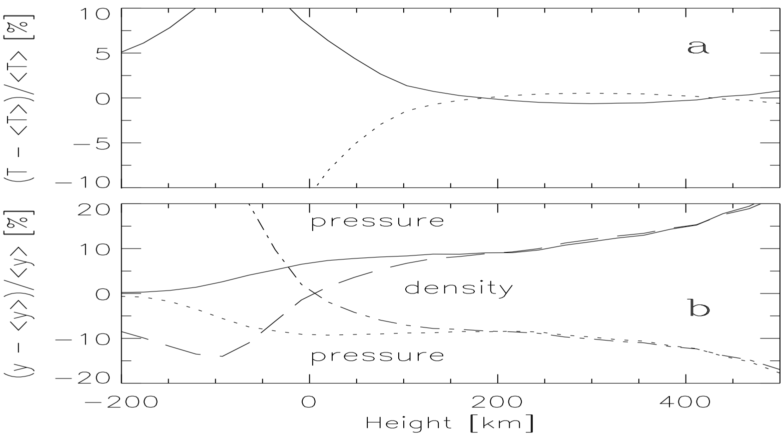

Fig. 1. Relative temperature (**a**), pressure and density (**b**) fluctuations in two-component representation: quantities were averaged over up- and downflows, separately. Temperature and gas pressure in upflows are shown by solid lines. Dotted lines are temperature and gas pressure in downflows. Dashed line is averaged density in upflows and dot-dashed line is mean density in downflows.

3. Theoretical correlative relationships

In this section we present height-dependent correlative relationships derived from 2-D models. In particular, we shall deal with two different sorts of correlations. The first of them is called a two-component representation, when thermodynamic quantities are averaged over up- and downflows, separately. Such relationships can be directly compared with the results, produced by inversion codes (Bellot Rubio et al. 1999, Frutiger et al. 1999, for instance). The second kind of correlations are linear correlation coefficients which reflect the linear dependence of model quantities between each other. These correlative dependencies were studied in a large number of papers using observations of spectral lines formed at various heights in the photosphere.

In this paper the surface level or $h = 0$ in the geometrical height scale corresponds to $\log \overline{\tau_R} = 0$, where $\overline{\tau_R}$ is the Rosseland optical depth spatially and temporally averaged over 2-D models.

3.1. Two-component representation

Figure 1 shows temperature, gas pressure and density averaged over up- and downflows, separately, over the total evolution time.

From Figure 1a we can clearly see two critical height levels where temperature fluctuations reverse their sign The first reversal (Nelson & Musman 1977) occurs at $h \sim 170$ km and is caused by cooling of thermal convective upflows which overshoot into stable photospheric layers and heating of downflows due to their compression. Near the traditional temperature minimum there exists the second reversal of temperature fluctuations – oscillating upflows are seen to be hotter again due to compression of the medium as they move into the upper atmospheric layers. Such behaviour of temperature fluctuations is very similar in 2-D models and in the output of inversion codes (Bellot Rubio et al. 1999, Frutiger et al. 1999).

Figure 1b exhibits the pressure and density averaged inside up- and downflows, separately, and shown as relative variations around their mean values at certain height levels. They outline three regions:

- convectively unstable subphotospheric layers (negative correlation between density and vertical velocity),
- a region of overshooting convection (correlation between density and vertical velocity becomes positive but $|\Delta P|/\overline{P}$ is significantly greater than $|\Delta\rho|/\overline{\rho}$ and $\Delta T/\overline{T}$ is positive (negative) in upflows (downflows),
- and oscillating photospheric layers being in radiative equilibrium ($\Delta P/\overline{P} \approx \Delta\rho/\overline{\rho}$).

Based on these models we may conclude that overshooting convection extends to about 150–170 km in the photosphere. The extent of the overshooting convection region, however, varies in dependence on the size of the convective cell: for instance, above cells with horizontal sizes of about 180 km it reaches up to 70–75 km (Gadun et al., 2000).

3.2. Correlative relationships

We shall analyse two kinds of correlations: two-point correlations, when correlation coefficients are defined between spatial fluctuations of model quantities derived at different heights in the model atmosphere – one point is fixed around the surface level and the other point will be taken at various heights. These correlations reflect changes in the columnar structure of the inhomogeneous atmosphere.

The next, one-point (local) correlations correspond to correlation coefficients calculated between spatial variations of model quantities at the same model layer.

The correlations between model quantities or line parameters were determined for each model or spectral scan. The mean correlation coefficients are being obtained by averaging over the modeling time interval or over the time interval of observations.

3.2.1. Two-point correlations

We start our analysis with correlations between δI (spatial variations of emergent monochromatic intensity at λ 500 nm) and spatial variations of temperature fluctuations at each horizontal level i in the photosphere (δT_i). They also demonstrate high correlation (Fig. 2) in the low photosphere, which drops rapidly with height and becomes even negative at h larger 120–130 km. This occurs due to the first reversal of temperature fluctuations inside the photospheric columnar structure (Fig. 1a): overcooling of the matter above the central part of the convective cell and heating of gas above intercellular lanes. The largest anticorrelation is found in the middle photosphere at heights between 250 and 350 km, where the reversal of temperature fluctuations is largest (Fig. 1a). At these heights the temperature fluctuations are almost a mirror image of the granular brightness field. In the upper photosphere this anticorrelation decreases but is still significant in spite of the second reversal of temperature fluctuations. This is because oscillations and shearing flows break down the quasi columnar structure there. In the Figures 2-4 we have used $n = 285$ models and for this reason the rms error will be far smaller than the standard deviation. In all these plots we show $x \pm \sigma$ values.

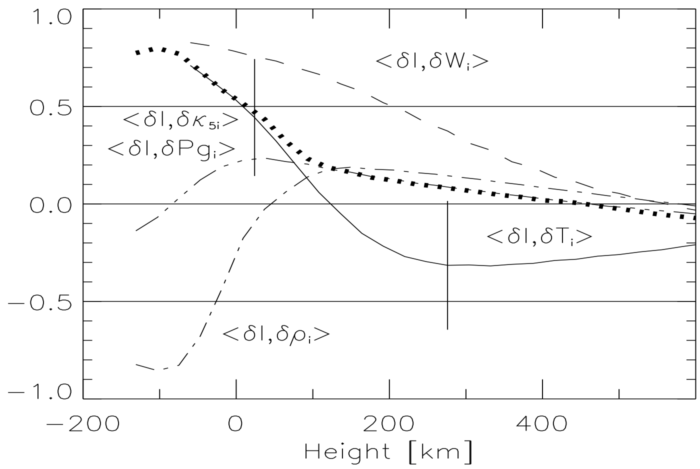

Fig. 2. Correlations between monochromatic emergent intensity at λ 500 nm and selected model quantities derived at various levels in the model photosphere. Error bars are estimates of standard deviations. The maximum rms error of correlation coefficients presented here is not larger than 0.03.

The correlation coefficients between δI and spatial variations of vertical velocities (δW_i) demonstrate another dependence on height: they decrease slowly from a high level of correlation in the low photosphere to almost zero level at or near the traditional temperature minimum. This means that reversal cells with granular scale sizes are not being formed in our model atmosphere – the reversal field of vertical velocities is not seen. The high correlation between δI and δW_i becomes smaller than 0.5 at a height of about 250 km.

$\langle \delta I, \delta Pg_i \rangle$ and $\langle \delta I, \delta \rho_i \rangle$ (correlations between δI and fluctuations of gas pressure and density, respectively) correspond to those as expected to be in the transition zone from thermal convection to layers with radiative equilibrium. For instance, $\langle \delta I, \delta \rho_i \rangle$ are in anticorrelation in subphotospheric layers – less dense matter is hotter and brighter as well, but in optically thin layers they become positive due to the buoyancy breaking effect.

The peak in height dependence of $\langle \delta I, \delta Pg_i \rangle$ is located around the surface, i.e. deeper than for the $\langle \delta I, \delta \rho_i \rangle$ stratification, and positive over almost the whole photosphere.

A behaviour of correlations between δI and $\delta \kappa_5$ (spatial variations of monochromatic opacity at λ 500 nm) seems to be very interesting. In the low photosphere, where temperature fluctuations are larger, they follow the $\langle \delta I, \delta T_i \rangle$ but in high photospheric layers $\delta \kappa_5$ almost coincides with spatial fluctuations of gas pressure. This is explained by the sensitivity of H^- ions to electron concentrations; H^- ions are the main absorber in the solar atmosphere. The electron concentration depends in the low photosphere mainly on hydrogen ionization which is strongly temperature-dependent, however in higher layers the metals are the main contributor. Since the metals are basically ionized due to the still high temperatures, the electron concentration in these layers is not very sensitive to temperature fluctuations.

In Figure 3 we present a series of two-point correlations in which we use a profile of vertical (δW_{-60}) and horizontal (δU_{-60}) velocities at 60 km depth below the surface instead of δI. They can serve as better indicators of the columnar structure of the model photosphere than correlations with δI.

Correlations with (δW_{-60}) show almost the same behaviour as the correlation coefficients with δI previously discussed. $\langle \delta W_{-60}, \delta T_i \rangle$, however, exhibit positive correlation over a larger geometrical height range than $\langle \delta I, \delta T_i \rangle$. It is important that horizontal velocities are highly correlated in these models over almost the whole photosphere. We note that from obvious reasons the correlation of spatial fluctuations of horizontal velocities with δI or δW_{-60} is absent (is close or equal to zero).

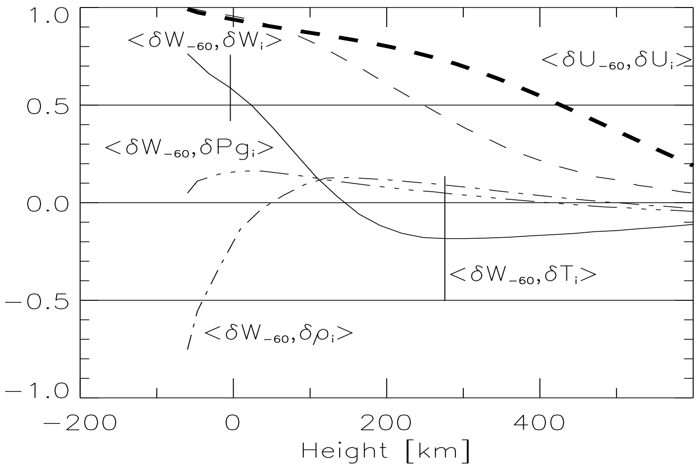

Fig. 3. Correlations between vertical velocity fluctuations at the depth 60 km below the surface and selected model quantities. Error bars are standard deviations. Maximum rms error of correlation coefficients shown here is not larger than 0.03.

3.2.2. One-point correlations

The one-point (local) correlations are given in Figure 4. They show the correlation coefficients found between selected model quantities for each horizontal level.

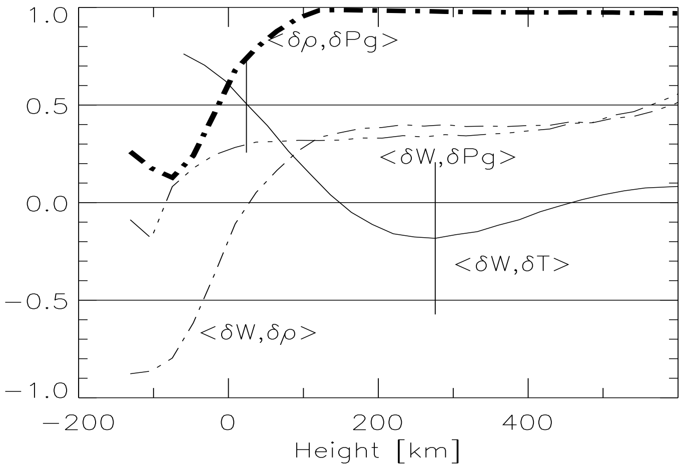

Fig. 4. Local correlations between spatial fluctuations of selected model quantities. Error bars are estimates of standard deviations. Maximum rms error of correlation coefficients presented here is not larger than 0.03.

$\langle \delta W, \delta T \rangle$ demonstrates, as mentioned above, two reversals of temperature fluctuations in the model atmosphere and a large anticorrelation due to overcooling of convective cells in optically thin layers. We may also note the relatively large positive correlations between vertical velocities and $\delta\rho$ and δPg: on the average, ascending flows produce denser atmospheric inhomogeneities which have higher pressure than downflows. $\delta\rho$ and δPg are highly correlated over the whole model atmosphere.

δW and $\delta\rho$ are negatively correlated up to a height about 30 km. This may serve as an argument that the top of thermal convection reaches the low photosphere. The same conclusion is followed from Figures 1-3.

Positive $\langle \delta W, \delta T \rangle$ in the upper photosphere does not change significantly the negative values of $\langle \delta I, \delta T_i \rangle$ and $\langle \delta W_{-60}, \delta T_i \rangle$ because the photosphere does not have a columnar structure there.

4. Comparison with line parameter correlations

Theoretical correlations $\langle \delta I, \delta T_i \rangle$, $\langle \delta I, \delta W_i \rangle$, and $\langle \delta W, \delta T \rangle$ can be compared with results of spectral observations made with high spatial resolution, namely with correlations $\langle \delta I, \delta r \rangle$, $\langle \delta I, \delta V \rangle$, and $\langle \delta V, \delta r \rangle$, if we suppose that a) we know exactly the region of the atmosphere where the spectral line is formed and b) if the region which contributes mainly to the line formation process is narrow. These both assumptions are supported by results of Kučera et al. (1998). Here δr denote spatial variations of residual intensity in the line core and δV correspond to spatial variations of Doppler shifts.

To test spectral lines in their ability to reproduce correctly the main real correlative relationships of the model photosphere we simulated spectral scans of 13 Fe I and 6 Fe II lines using our time-dependent 2-D models. The line parameters are given in Table 1. Together with line wavelength (λ) and low excitation potential (EPL), Table 1 represents an estimation of line formation heights. H_{ew} is effective height of line formation for the line equivalent width (weighted over the whole profile); H_d is the effective height of line formation for central line depth; H_τ is the geometrical height at line center optical depth $\tau_{\lambda 0} = \tau^{c+l}_{\lambda 0} = 1.0$. Here $\tau^{c+l}_{\lambda 0}$ denote the integral optical depth in the line and in the continuum at the wavelength of the line center. H_{ew} and H_d were calculated with depression contribution and Unsöld-Pecker weighting functions. All these weighting quantities we computed for a 1-D model which was obtained by spatially and temporally averaging our sequence of 2-D models presented here.

Figure 5 displays the theoretical correlations, derived from simulated spectral scans of lines, which are shown in dependence on H_d (Fig.5 a–c) and H_τ (Fig.5d–f). If we compare between $\langle \delta I, \delta W_i \rangle$ and $\langle \delta I, \delta V \rangle$ (Fig.2 – Fig.5 a and d), $\langle \delta W, \delta T \rangle$ and $\langle \delta V, \delta r \rangle$ (Fig.4 – Fig.5 b and e), and $\langle \delta I, \delta T_i \rangle$ and $\langle \delta I, \delta r \rangle$ (Fig.2 – Fig.5c and f) it is easy to conclude that a) spectral line correlations are correctly reproducing real correlative relationships of the model atmosphere if b) we use the H_τ scale of geometrical heights for our sample of spectral lines. So, this scale is more suitable for diagnostic purpose in the context of our 2-D models.

To test these theoretical correlations we present in Figs.5 g–i correlation coefficients calculated for five Fe I lines from spectral observations described in Sect. 2.

Table 1. Parameters of the spectral lines used for the simulation of the spectral scans from the time-dependent model.

λ Å	El.	EPL eV	H_d km	H_{ew} km	H_τ km
4911.536	Fe I	4.26	148	126	45
6494.499	Fe I	4.73	155	131	71
6495.740	Fe I	4.83	165	132	89
4911.782	Fe I	3.93	181	148	121
5679.032	Fe I	4.65	197	151	158
6496.472	Fe I	4.79	204	155	162
5543.944	Fe I	4.22	215	168	183
6027.059	Fe I	4.07	230	174	185
6481.878	Fe I	2.28	266	217	222
6280.622	Fe I	0.86	303	246	253
5250.216	Fe I	0.12	330	277	308
5250.654	Fe I	2.20	352	292	406
6494.994	Fe I	2.40	414	308	492
5136.800	Fe II	2.84	94	84	23
5100.656	Fe II	2.81	99	85	32
5425.259	Fe II	3.20	128	105	89
6432.683	Fe II	2.89	141	115	89
4576.339	Fe II	2.84	186	148	177
5234.630	Fe II	3.22	238	176	233

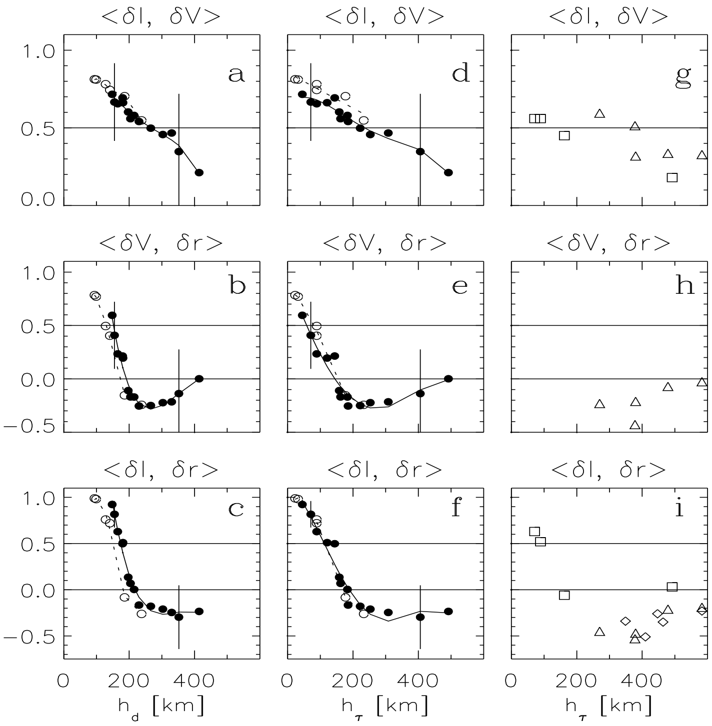

Fig. 5. Theoretical correlations found from simulated (**a**–f) and observed (**g**–**i**) spectral scans. Error bars are estimates of the standard deviations – they reflect a scatter of correlation coefficients measured from the set of spectrograms. Open circles and dashed lines present Fe II lines, filled circles with solid lines are correlations obtained with Fe I lines. Squares stem from Fe I observations of Hanslmeier et al. (1990); triangles from Fe I observations of Kučera et al. (1995) and those presented here; and diamonds from Fe I lines investigated by Balthasar et al. (1990).

We selected observations from purely quiet regions for this comparison. They are free from any network activity. Numerical values of correlations are given in Table 2 where means and differences have been derived from two subsequent exposures taken in the same slit position. H_τ height, determined in the same way as in Table 1, is given in Tab.2 also. Moreover in Figs.5 g–i some previously published data are added from papers of Hanslmeier et al. (1990), Balthasar et al. (1990), and Kučera et al. (1995).

Although the observations do not describe possible relationships in detail, they are not in disagreement with the theoretical prediction. Very important is that $\langle \delta V, \delta r \rangle$ show a tendency to decrease their negative correlative relationship in the upper photosphere in agreement with model predictions.

Table 2. Correlations of the spectral line characteristics derived from two measurements of five Fe I lines.

λ Å	H_τ km	$\langle \delta I, \delta V \rangle$	$\langle \delta V, \delta r \rangle$	$\langle \delta I, \delta r \rangle$
6302.499	270	0.60±0.08	−0.23±0.06	−0.45±0.03
6301.508	378	0.51±0.10	−0.43±0.06	−0.53±0.06
5576.099	380	0.32±0.09	−0.21±0.07	−0.47±0.05
6494.994	492	0.34±0.12	−0.07±0.14	−0.21±0.16
5434.543	583	0.33±0.13	−0.03±0.13	−0.19±0.13

5. Discussion and conclusion

The height variation of the model correlations changes if we use another way to calculate mean correlation coefficients: we may collect data belonging to each horizontal level over a whole time series of our models and calculate then correlations between these data. But the height dependencies of the new correlations differ from those discussed in this paper not more than by 20–30 km and this does not change dramatically our main conclusions.

From our simulated spectral scans we do not detect the sharp drop of correlation between spatial fluctuations of vertical velocities in the low and in the middle photosphere as was reported by Karpinsky (1990). An explanation can be that our models are obviously more laminar than the real solar photosphere. However, this conclusion of Karpinsky was not confirmed later.

Our results with high coherence between horizontal velocities in the model photosphere are also in disagreement with a study of Nesis et al. (1988), where they found, based on observations, that horizontal velocities are coherent only in the low photosphere. Probably our 2-D and close to laminar treatment of thermal convection and oscillations in the spatially limited computational domain may influence the behaviour of the velocity field and especially its horizontal component. These may provoke such a highly coherent behaviour of the horizontal velocities in the models.

In spite of this the correlations derived from observations and from simulations of several Fe I and Fe II lines are in good agreement. Therefore, summarizing our results we may conclude that
a) in the whole photosphere above granules the matter predominantly ascends. In the middle and upper photosphere, the downward directed component of oscillations is less intense above granules compared with regions above intergranular lanes. This can be expalined by wave oscillating phenoma;
b) clouds of cold and dense matter are located above bright granules beginning from heights about 150–170 km;
c) the columnar structure of photosphere is destroyed beginning from ∼250 km.

Schematically, the structure of the model photosphere can be presented as the following:
a) low photosphere: it seems that the top of the thermal convection zone lays at 20–50 km above the visible surface;
b) then we have convection overshoot into stable layers up to 150–170 km;
c) between 170 and 250–300 km we detect a transition layer where the convective columnar structure still exists, due to the influence of convective pressure variations, and where the inversion of temperature fluctuations is largest;
d) above 300 km this columnar structure is broken on the average and the photospheric medium is controlled mostly by oscillations.

This scheme agrees with the picture from spectral observations (Nesis et al. 1988, Karpinsky 1990).

Finally we point out that multidimensional selfconsistent model atmospheres can be successfully used to test possible criteria in estimation of "line formation depths". Although our results show that H_τ scale seems to be better for diagnostic purpose than line formation depths found with depression contribution functions we suggest to test also physically more adequate methods using conception of response functions.

Acknowledgements. A. G. and A. H. thank the Austrian Academy of Sciences and National Academy of Sciences of Ukraine for financing the exchange of scientists. A. H. thanks the 'Austrian Fonds zur Förderung der wissenschaftlichen Forschung' for supporting these investigations. A. K and J. R. acknowledge the grant VEGA 2/7229/20 and the Austrian and Slovak Academy of Sciences.

References

Balthasar H., Grosser H., Schröter C., Wiehr E., 1990, A&A 235, 437
Bellot Rubio L.R., Ruiz Cobo B., Collados M., 1999, A&A 341, L31
Canfield R.C., Mehltretter J.P., 1973, Solar Phys. 33, 33
Durrant C.J., Nesis A., 1981, A&A 95, 221
Durrant C.J., Nesis A., 1982, A&A 111, 272
Evans J.W., 1964, Astroph. Norveg. 9, 33
Frutiger C., Solanki S.K., Bruls J.H.M.J., Fligge M., 1999, In: Solar Polarization, Nagendra K.N. and Stenflo J.O. (Eds.), Kluwer, Dordrecht, in press
Gadun A.S., Solanki S.K., Johannesson A., 1999, A&A 530, 1018
Gadun A.S., Hanslmeier A., Pikalov K.N., 1997, A&A 320, 1001
Gadun A.S., Ploner S.R.O., Hanslmeier A., Pikalov K.N., Puschmann K.G., Solanki S.K., 2000, A&A, in preparation (also Gadun A.S., Solanki S.K., Ploner S.R.O., Hanslmeier A., Pikalov K.N., Puschmann K.G., 1998, Size-Dependent Properties of 2-D Artificial Solar Granulation, Main Astr. Obs., Kiev, preprint no. MAO-98-4E)
Hanslmeier A., Mattig W., Nesis A., 1990, A&A 238, 345
Hanslmeier A., Nesis A., Mattig W., 1994, A&A 288, 960
Hanslmeier A., Kučera A., Rybák J., Neunteufel B., Wöhl H., 2000, A&A, in press
Karpinsky V.N., 1990, In: Solar Photosphere: Structure, Convection, and Magnetic Fields, Stenflo J.O. (Ed.), Kluwer, Dordrecht, p. 67
Keil S.L., Canfield R.C., 1978, A&A 70, 169
Kneer F.J., Mattig W., Nesis A., Werner W., 1980, Solar Phys. 68, 31
Komm R., Mattig W., Nesis A., 1990, A&A 239, 340
Komm R., Mattig W., Nesis A., 1991a, A&A 243, 251
Komm R., Mattig W., Nesis A., 1991b, A&A 252, 812
Krat V.A., 1973, Solar Phys. 32, 307
Kučera A., Rybák J., Wöhl H., 1995, A&A 298, 917
Kučera,A., Balthasar, H., Rybák, J., Wöhl, H., 1998, A&A, 332, 1069
Leighton R.B., Noyes R.W., Simon G.W., 1962, ApJ 135, 474
Nelson G.D., Musman S., 1977, ApJ 214, 912
Nesis A., Durrant C.J., Mattig W., 1988, A&A 201, 153

This article was processed by the author using Springer-Verlag LaTeX A&A style file *L-AA* version 3.